


## Inverse Cascade Spectrum of Gravity Waves in the Presence of a Condensate: A Direct Numerical Simulation

Alexander O. Korotkevich <sup>\*</sup>

*Department of Mathematics and Statistics, University of New Mexico,  
MSC01 1115, 1 University of New Mexico, Albuquerque, New Mexico 87131-0001, USA  
and L.D. Landau Institute for Theoretical Physics RAS, Prospekt Akademika Semenova 1A,  
Chernogolovka, Moscow region, 142432, Russian Federation*



(Received 29 November 2022; accepted 30 May 2023; published 28 June 2023)

During the set of direct numerical simulations of the forced isotropic turbulence of surface gravity waves in the framework of primordial dynamical equations, the universal inverse cascade spectrum was observed. The slope of the spectrum is the same (in the margin of error) for different levels of pumping and nonlinearity as well as dissipation present in the system. In all simulation runs formation of the inverse cascade spectrum was accompanied by the appearance of a strong long wave background (condensate). The observed slope of the spectrum  $\sim k^{-3.07}$  is different from the constant wave action flux solution predicted by the wave turbulence theory  $\sim k^{-23/6}$ .

DOI: [10.1103/PhysRevLett.130.264002](https://doi.org/10.1103/PhysRevLett.130.264002)

*Introduction.*—The waves turbulence theory (WTT) (see, e.g., Refs. [1,2]) describes the evolution of a distribution function for weakly nonlinear waves. One of the most important applications of WTT is wave forecasting: a statistical description of evolution of the wave field in a sea or an ocean. Most of the current operational wave forecasting models are based either directly on Hasselmann waves kinetic equation [3] (WKE) for surface gravity waves (when one neglects capillary effects) with extra phenomenological terms or on its variations [4,5]. Thus, verification of the applicability of WKE for different setups is an important practical question. Two constant flux solutions of WKE for gravity waves, corresponding to direct [6] and inverse [7] cascades, were found by Zakharov and coauthors [1,2,8]. These Kolmogorov-Zakharov (KZ) solutions are formulated for inertial intervals: ranges of scales where dynamics is determined by the nonlinear interaction of waves, and direct influence of dissipation or pumping is negligible. If one could confirm the observation of these solutions in a field, laboratory, or numerical experiment, this would be a strong argument in support of the applicability of WKE in particular conditions.

While the spectrum corresponding to the direct cascade of energy to small scales was observed both experimentally [9,10] and numerically [11–15], the inverse cascade spectrum of wave action from smaller to larger scales appeared to be a harder case. Although frequency downshift, which can be explained by inverse cascade, was observed in direct numerical simulations (DNSs) of decaying turbulence (evolution of initial spectrum without forcing in the system) [11,16–18], it could not be a substitute for the inverse

cascade spectrum, which can be obtained only in the case of forced turbulence. Perhaps, the first attempt toward this goal was Ref. [19], where the initial stage of the formation of the KZ-spectrum was demonstrated, but the range of scales with a powerlike spectrum was not sufficient to determine the slope. The attempt to observe both inverse and direct cascades simultaneously [20] has resulted in the formation of an inverse cascade and a *condensate* (strong long wave background), which affected even the direct cascade spectrum, but the range of scales in the inverse cascade region was again insufficient to determine the slope accurately enough. A description of some of the laboratory experiments, where an observation of inverse cascade was attempted, can be found in Ref. [21]. The major problem in early attempts [22] was the small size of the basin which required one to excite waves in the capillary-gravity crossover region [23]. Even in later experiments in a relatively large wave tank [24], both the dynamical range and finite size effects prevented clear observation of the slope of the inverse cascade. In all numerical and at least some of the laboratory experiments mentioned above formation of the condensate was observed (although, not always noted).

The importance of condensate influence upon the gravity waves spectrum was demonstrated in Ref. [20] and investigated in details in Ref. [25]. At least one of the important mechanisms of the condensate formation is the arrest of the nonlinear interactions due to discreteness of the homogeneous wave numbers grid, typical for both DNS with periodic boundary conditions and relatively small laboratory basins, like in Ref. [22]; thus the condensate is not

purely a numerical artifact. The importance of discreteness of the wave numbers grid for nonlinear interactions was noted a long time ago for waves in resonators [26,27] and investigated in detail with direct application to WTT [15,28–30]. Although there are exact resonances present on a discrete homogeneous grid of wave vectors [31], the quasiresonances due to nonlinear broadening of the resonance curve play a very important role for turbulent fluxes in simulations of WTT [32]. As the inverse cascade spectrum propagates further from the pumping region to the smaller wave numbers (larger scales), eventually nonlinear interaction through quasiresonances is arrested by the discreteness and the flux only brings wave action without further propagation, resulting in the accumulation of it at some large scale [20,25,33] (a similar phenomenon was observed for direct cascade in Ref. [34]). This results in the formation of a strong (an order of magnitude larger than even closest harmonics) long wave background, which we call condensate. The powerlike inverse cascade spectrum can be observed in the inertial interval between condensate and pumping regions, like in laboratory experiments [21,22] or in DNS [19,20]. In these simulations the inertial interval was too short to allow one to determine the slope of the inverse cascade with reasonable accuracy and compare it with the WTT prediction. Taking into account the extremely slow formation of the inverse cascade (meaning a smaller resolution for faster computations) and necessity of a reasonable dynamic range for determining the slope of the spectrum, one needs to find a compromise between these contradicting requirements.

In this Letter we present results of DNSs in the framework of primordial dynamical equations of the forced turbulence of surface gravity waves and formation of the inverse cascade with a powerlike spectrum. Simulations were performed for different levels of pumping, resulting in different nonlinearity levels and different parameters of dissipation, for an extremely long ( $\approx 10^6$  periods of central pumping harmonic) period of time. In all the cases we obtained condensate formation and were able to determine the slope of the inverse cascade spectrum, virtually the same for all simulations, yet different from one predicted by WTT. The new spectrum is simultaneously a challenge for WTT, a more detailed set of data supporting some experiments, and a stimulus for new breakthroughs in theory.

*Problem formulation.*—We consider a potential flow (velocity of the fluid is  $\mathbf{v} = \nabla\Phi$ ) of an ideal incompressible fluid of infinite depth. Elevation of the 2D surface over 3D fluid from the steady state is described by a function  $\eta(\mathbf{r}; t)$ , where  $\mathbf{r} = (x, y)^T$  is the coordinate vector in a horizontal plane. The velocity potential on the surface is  $\psi(\mathbf{r}; t) = \Phi|_{z=\eta(\mathbf{r}; t)}$ . The system is Hamiltonian [35] with respect to variables  $\eta$  and  $\psi$ . An average slope of the surface  $\mu = \sqrt{\langle |\nabla\eta(\mathbf{r})|^2 \rangle}$ , also called steepness, in most of the observations is a small parameter  $\mu \ll 1$ . One can expand

the Hamiltonian in powers of  $\mu$  (see Sec. I of the Supplemental Material [36]) and obtain Hamiltonian equations:

$$\begin{aligned} \dot{\eta} &= \hat{k}\psi - [\nabla(\eta\nabla\psi)] - \hat{k}[\eta\hat{k}\psi] \\ &\quad + \hat{k}(\eta\hat{k}[\eta\hat{k}\psi]) + \frac{1}{2}\Delta[\eta^2\hat{k}\psi] + \frac{1}{2}\hat{k}[\eta^2\Delta\psi] - F^{-1}[\gamma_k\eta_k], \\ \dot{\psi} &= -g\eta - \frac{1}{2}[(\nabla\psi)^2 - (\hat{k}\psi)^2] \\ &\quad - [\hat{k}\psi]\hat{k}[\eta\hat{k}\psi] - [\eta\hat{k}\psi]\Delta\psi - F^{-1}[\gamma_k\psi_k] + F^{-1}[f_k]. \end{aligned} \quad (1)$$

Artificial pumping and damping terms will be described later in Eq. (5). Here  $\hat{k}$  is a linear integral operator  $\hat{k} = \sqrt{-\Delta}$ , such that  $\hat{k}f_{\mathbf{r}}$  in  $k$  space corresponds to multiplication of Fourier (in the horizontal  $XY$  plane) coefficients  $f_{\mathbf{k}}$ :

$$\begin{aligned} \hat{F}[f_{\mathbf{r}}] &= f_{\mathbf{k}} = \frac{1}{L_x L_y} \int_0^{L_x} \int_0^{L_y} f_{\mathbf{r}} e^{-i\mathbf{k}\mathbf{r}} d\mathbf{r}, \\ \hat{F}^{-1}[f_{\mathbf{k}}] &= f_{\mathbf{r}} = \sum_{\mathbf{k}} f_{\mathbf{k}} e^{i\mathbf{k}\mathbf{r}} \end{aligned}$$

by  $k = |\mathbf{k}| = \sqrt{k_x^2 + k_y^2}$ . For gravity waves these reduced Hamiltonian equations describe four-wave interaction. In the case of a statistical description of the wave field, WKE for the distribution of wave action  $n(k, t) = \langle |a_{\mathbf{k}}(t)|^2 \rangle$  is used. Here

$$a_{\mathbf{k}} = \sqrt{\omega_k/(2k)}\eta_{\mathbf{k}} + i\sqrt{k/(2\omega_k)}\psi_{\mathbf{k}}, \quad (2)$$

are complex normal variables. For gravity waves  $\omega_k = \sqrt{gk}$ . More precisely, one has to use a different function  $b_{\mathbf{k}}$  after canonical transformation eliminating nonresonant cubic terms [1,2] in the Hamiltonian, but the relative difference between corresponding  $n_k$ 's in the case of  $\mu \approx 0.1$  is of the order of a few percent, so we shall limit ourselves by a simpler function [Eq. (2)].

From WTT [1,2], in the case of four-wave interaction (typical for surface gravity waves), besides equipartition spectra, under few reasonable assumptions, one can find two constant flux KZ solutions [6,7,37] of WKE:

$$n_k^{(1)} = C_1 P^{1/3} k^{-\frac{2\beta}{3}-d}, \quad n_k^{(2)} = C_2 Q^{1/3} k^{-\frac{2\beta-\delta}{3}-d}. \quad (3)$$

For surface gravity waves, a coefficient of homogeneity of nonlinear interaction coefficient  $\beta = 3$ , the power of dispersion law  $\delta = 1/2$ , and the dimension of the surface  $d = 2$ . As a result we get

$$n_k^{(1)} = C_1 P^{1/3} k^{-4}, \quad n_k^{(2)} = C_2 Q^{1/3} k^{-23/6}. \quad (4)$$

The solution  $n_k^{(1)}$  describes a direct cascade of energy from large pumping to small dissipative scales and was observed

in simulations [11–13,20]. The second spectrum  $n_k^{(2)}$  describes an inverse cascade of wave action from small pumping to larger scales.

*Numerical scheme parameters.*—We simulate Eq. (1) in a (double) periodic box  $L_x = L_y = 2\pi$ . Grid resolution  $N_x = N_y = 512$ .

Pumping on large scales [term with  $f_k$  in Eq. (1)] and dissipation on small scales (terms with  $\gamma_k$ ) are

$$f_k = 4F_0 e^{iR_k(t)} \frac{(k - k_{p1})(k_{p2} - k)}{(k_{p2} - k_{p1})^2};$$

$$\gamma_k = \begin{cases} \gamma_0(k - k_d)^2, & k \geq k_d, \\ \gamma_k = 0, & k < k_d. \end{cases} \quad (5)$$

The pumping parameters  $F_0 = 5 \times 10^{-9} (\times 2, \times 4, \times 8)$ ,  $k_{p1} = 60$ , and  $k_{p2} = 64$ , i.e., for four different simulation runs the amplitude  $|F_0|$  was differing by factors  $\times 2$ ,  $\times 4$ , and  $\times 8$  from the smallest one. Function  $f_k$  is a parabola with zeros at  $k_{p1}$  and  $k_{p2}$  and extremum equal to  $|F_0|$  in the middle  $k_p = 62$  between them;  $f_k$  is zero outside of an interval  $k \in [k_{p1}; k_{p2}]$ .  $R_k(t)$  is a uniformly distributed random number in the interval  $(0, 2\pi]$ , different for every harmonic and time step. Initial amplitudes for all  $\eta_k$  and  $\psi_k$  harmonics were  $10^{-12}$ , and all phases were uniformly distributed random numbers between  $(0, 2\pi]$ . Damping starts at  $k_d = 128$  and zero for larger scales (to avoid the influence of aliasing due to cubic nonlinearity in our equations, we suppress harmonics with  $k > k_{\max}/2$ , where  $k_{\max} = 256$ ). Following Ref. [38] damping has to be included in both equations of Eq. (1). The value of  $\gamma_0$  was chosen automatically to ensure 6 orders of harmonics magnitude difference between the center of the pumping region  $k_p = 62$  and the last Fourier harmonics at  $k = k_{\max}$ . It guarantees good quality of the solution in spite of the fact that the Fourier series is being truncated. Later, after formation of the condensate, the difference of the largest and smallest (in magnitude) harmonics reaches 7 orders of magnitude. It should be noted, that the values of  $\gamma_0$  were different for different levels of pumping as different fluxes of energy to the high  $k$ 's had to be dissipated. Details of the numerical algorithm can be found in Ref. [30]. FFTW library [39] was used as a discrete Fourier transform implementation.

In the  $k$ -space supports of  $\gamma_k$  and  $f_k$  are separated by the inertial interval, where the KZ solution corresponding to the direct cascade of energy could be recognized, but the range of scales in this set of numerical simulations was insufficient. Another inertial interval is located between  $k = 0$  and the pumping region; here we expected to observe inverse cascade. Because both dissipation and pumping are isotropic (except for random phases) with respect to the polar angle, we expect the same property for a solution, and we use it for averaging the resulting spectra to replace ensemble averaging.

Computations were performed on a designated CPU core for each value of  $F_0$  and took more than a year. This is the reason for a relatively small grid resolution, even with respect to our previous computations [13,20,25]. During previous works it had become clear that formation of the inverse cascade is an extremely slow process, which is explained by the fact that the interaction coefficient for gravity waves behaves as  $\sim k^3$ , which means that interaction slows quickly with a decrease of  $k$ . Also, in weakly nonlinear approximation characteristic nonlinear time  $T_{nl}$ , when nonlinearity shows itself (amplitude change of order 1), has to be much more than a period corresponding to linear dispersion  $T_k = 2\pi/\omega_k$ , while linear frequency  $\omega_k$  also decays with a decrease of  $k$ . In order to avoid a direct drain of energy from the pumping region through slave harmonics, we had to ensure that only third harmonic ( $3k_{p2}$ ) of pumping is in the dissipation region (see Ref. [40]). Simultaneously, we had to leave room for inverse cascade development. Taking into account all these considerations and the enormous time of the inverse cascade formation (we had to compute till times  $> 10^6 T_p$ , where  $T_p = 2\pi/\omega_{k_p}$ ), the relatively small resolution  $512 \times 512$  was a reasonable compromise.

*Numerical results.*—The computations were performed until a time close to a million of periods of a harmonic at the maximum of pumping  $T_p$ . As a replacement of ensemble averaging, which is unfeasible taking into account the computation time, in order to compute  $n_k = \langle |a_k|^2 \rangle$  we used averaging over an angle as the situation is isotropic and pumping has a random phase in every harmonics and at every moment of time. There are more harmonics to average over in larger  $k$ 's, meaning fewer fluctuations of  $\langle |a_k|^2 \rangle$ . The resulting mean steepnesses  $\mu$  for all four cases were 0.054, 0.067, 0.093, and 0.135. It should be noted that these values correspond to a very different dissipation due to nonlinear processes, as was shown in Refs. [41,42] (see Ref. [43]). The obtained angle averaged spectra are shown

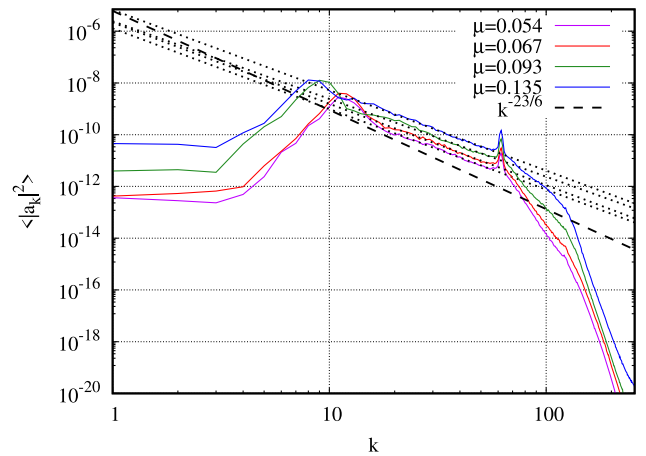


FIG. 1. All simulation spectra (solid lines) with corresponding least squares fits (dotted lines, values of slopes are given in Table I) and KZ-spectrum slope (dashed line).

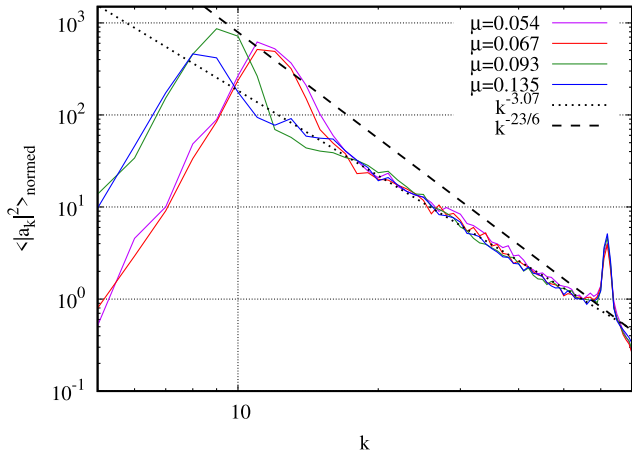


FIG. 2. All simulation spectra (solid lines) normed to have a value of  $\langle |a_k|^2 \rangle$  at  $k = 55$  to be 1 with a least squares fits (dotted line; value of the slope is given in Table I) over data points between condensate and pumping regions for all spectra and KZ-spectrum slope (dashed line).

in Fig. 1. In accordance with the theory in Ref. [30], the width of the resonant curve, necessary for working quasiresonances, depends on the nonlinearity in the system, resulting in further propagation of the inverse cascade and condensate for higher levels of steepness. For scales between regions influenced by condensate and pumping, we observe powerlike spectra (shown by dotted lines), with slopes practically independent of steepness. As one can see from Fig. 1, the higher the nonlinearity level is, the longer the inertial interval is, where a powerlike spectrum can be observed. This universal spectrum has a slope which is even visually different from the KZ spectrum  $\sim k^{-23/6} \approx k^{-3.83}$ . The slopes' values together with intervals used for linear least squares fit (in double logarithmic representation, like in Fig. 1) are given in Table I. The least squares fit was performed both in the OCTAVE [44] (part of GNU PROJECT [45]) package (via standard QR approach) and in GNUPLOT [46] (via Marquardt-Levenberg algorithm); standard errors [47] are from the Gnuplot computations. The slopes are significantly different from  $-23/6 \approx -3.83$  in accordance

TABLE I. Least squares fits for different simulation spectra. The second column shows the range of  $k$  between the condensate and pumping influenced regions; the third column gives the average slope  $\alpha$  for  $\langle |a_k|^2 \rangle \sim k^\alpha$ ; the last column shows an estimated error of the fit.

$\mu$	$k \in$	Average slope	Slope error
0.054	[17;55]	-3.12	$\pm 0.04$
0.067	[16;55]	-3.14	$\pm 0.05$
0.093	[12;56]	-3.01	$\pm 0.05$
0.135	[11;56]	-3.11	$\pm 0.04$
All	170 points	-3.07	$\pm 0.02$

with Fig. 1. To better understand the universality of the observed inverse cascade spectrum, we normalized all results in order to make an amplitude of  $|a_k|^2$  of the harmonic  $k = 55$  (see Ref. [48]) equal to 1. As a result, all spectra collapsed to a single curve (line) in the inertial interval (up to fluctuations due to insufficient averaging), shown in Fig. 2. We used the set of all available points in inertial intervals for all simulation runs for a least squares fit. The resulting slope is given in the last line of Table I and shown as a dotted line in Fig. 2. The value of the estimated spectrum slope is  $\langle |a_k|^2 \rangle \sim k^{-3.07}$ , which is again, expectedly, different from the one predicted by WTT [see Eq. (4)]. The reason for this inconsistency is yet to be found (e.g., see Ref. [49]).

It also can be noted that Fig. 2 strongly resembles Fig. 3 in Ref. [19], with the difference that we performed four different simulations and have a significantly longer inertial interval for inverse cascade allowing us to determine the slope with reasonable accuracy. The slopes in Table I with given errors margins have a point of intersection for all but one simulation runs (see Ref. [52]), corresponding to the slope  $-3.09$ . Thus, one can conclude that the slope is roughly between  $-3.0$  and  $-3.1$ , and probably closer to the  $-3.1$  value. Nevertheless, the difference between observed slope and the one predicted by WTT is clear both visually and numerically.

*Conclusion.*—During four numerical simulations with different pumping and dissipation parameters, we observed the formation of the inverse cascade and the condensate. In the inertial interval between condensate and pumping regions the universal spectrum is close to a powerlike function with a least square fit suggesting  $\sim k^{-3.07}$  slope. This is close to an experimentally observed spectrum in recent wave tank experiments [21] (see Fig. 12 (right) where our  $n_k \sim k^{-3.07}$  would correspond to  $E_k \sim k^{-1.57}$ , close to the  $E_k \sim k^{-1.5}$  proposed in that work), especially taking into account relatively noisy experimental data and a short range of scales. The slope of the spectrum is virtually identical for dramatically different levels of nonlinearity, which suggests the universality of the observed solution. Regardless of the fact that the spectrum is significantly different from the one predicted by WTT, the dependence of a constant in front of the powerlike function on the pumping parameters was investigated (see Sec. II of the Supplemental Material [36]). It was shown that at least in the first (linear) approximation the dependence of the constant on the flux is in reasonable agreement with Eq. (4), namely with  $Q^{1/3}$ , which hints that the new spectrum is a result of four-wave interaction.

The applicability of WKE (which is derived for an infinite domain) to DNS in a periodic box is yet to be investigated in detail. Recent works on the 3D nonlinear Schrödinger equation (NLSE) [53] and 1D quintic NLSE [54] give us hope that a precise range of simulation parameters, when one could expect quantitative

correspondence between WKE and DNS of dynamical equations for surface gravity waves, will be determined in future works. For now we could use previous simulations [11,13,17,20,32] as empirical evidence that one could expect at least qualitative correspondence (spectra slopes, spectrum peak downshift, etc.) for simulations in the frameworks of these significantly different models.

The constant wave action flux KZ spectrum  $\sim k^{-23/6}$  was derived for a particular case (infinite inertial interval, one spectrum in the whole range of wave numbers, etc.), which is different from what we observe in our simulations and experiments (finite range of scales, limited both by condensate and pumping). Similarly, the direct cascade of the energy KZ spectrum was not always observed in wave tank experiments [55,56], while in the open water in most of the cases [9,10] the KZ spectrum is observed. An explanation of the spectrum reported in this Letter is yet to be proposed, although previous works [20,25,33] hint that the condensate plays a major role for processes in the inverse cascade inertial interval. In order to take into account the condensate, one could use several different approaches: Bogolyubov transformation, similar to the technique used in a recent work [57]; taking into account the bottleneck phenomenon as was done in Ref. [58] for 2D turbulence; subtracting the condensate as in Refs. [59,60]; and studying the spectrum of remaining fluctuations. A lot depends on the type of the condensate. If it is a coherent structure, the approaches listed above could be applied. As the condensate is a ring with a radius between 8 and 15 for different simulations with a width around several harmonics, the total number of discrete harmonics in condensate is more than 100, and if they are stochastic enough (this is yet to be defined) the situation could be described by WKE [61]. In all of these cases complexity of the interaction coefficient (e.g., see Appendix B in Ref. [62]) for surface gravity waves makes analysis difficult enough to be a topic of a separate investigation. The final  $\eta(\mathbf{r})$  and  $\psi(\mathbf{r})$  surfaces for all four runs can be downloaded in the Supplemental Material [36]. Description of the file format is given in Sec. III of the Supplemental Material [36].

The author is grateful for support from the Simons' Collaboration on Wave Turbulence (Award No. 651459). The simulations presented in this article were performed using the Landau Institute for Theoretical Physics computational resources. The Letter was written during the author's visit to the Université Côte d'Azur/Institut de Physique de Nice, France, funded by Fédération de Recherche "Wolfgang Döblin" and "Waves Complexity" visiting researcher program, to whom the author is thankful for hospitality and support. The author would also like to thank V. V. Lebedev and I. V. Kolokolov for stimulating discussions.

\* alexkor@math.unm.edu

[1] V. E. Zakharov, V. S. Lvov, and G. Falkovich, *Kolmogorov Spectra of Turbulence I* (Springer-Verlag, Berlin, 1992).

- [2] S. V. Nazarenko, *Wave Turbulence* (Springer-Verlag, Berlin Heidelberg, 2011).
- [3] K. Hasselmann, *J. Fluid Mech.* **12**, 481 (1962).
- [4] G. J. Komen, L. Cavaleri, M. Donelan, K. Hasselmann, and P. A. E. M. Janssen, *Dynamics and Modelling of Ocean Waves* (Cambridge University Press, Cambridge, UK, 1994).
- [5] L. Cavaleri *et al.*, *Progr. Oceanogr.* **75**, 603 (2007).
- [6] V. E. Zakharov and N. N. Filonenko, *Sov. Phys. Dokl.* **11**, 881 (1967).
- [7] M. M. Zaslavskii and V. E. Zakharov, *Izv. Akad. Nauk SSSR Fiz. Atm. i Okeana* **18**, 747 (1982).
- [8] V. E. Zakharov, in *Breaking Waves*, edited by M. L. Banner and R. H. J. Grimshaw (Springer Berlin Heidelberg, Berlin, Heidelberg, 1992) pp. 69–91.
- [9] M. A. Donelan, J. Hamilton, and W. H. Hui, *Phil. Trans. R. Soc. A* **315**, 509 (1985).
- [10] P. A. Hwang, D. W. Wang, E. J. Walsh, W. B. Krabill, and R. N. Swift, *J. Phys. Oceanogr.* **30**, 2753 (2000).
- [11] M. Onorato, A. R. Osborne, M. Serio, D. Resio, A. Pushkarev, V. E. Zakharov, and C. Brandini, *Phys. Rev. Lett.* **89**, 144501 (2002).
- [12] A. I. Dyachenko, A. O. Korotkevich, and V. E. Zakharov, *JETP Lett.* **77**, 546 (2003).
- [13] A. I. Dyachenko, A. O. Korotkevich, and V. E. Zakharov, *Phys. Rev. Lett.* **92**, 134501 (2004).
- [14] N. Yokoyama, *J. Fluid Mech.* **501**, 169 (2004).
- [15] Y. Lvov, S. V. Nazarenko, and B. Pokorni, *Physica (Amsterdam)* **218D**, 24 (2006).
- [16] V. E. Zakharov, A. O. Korotkevich, A. Pushkarev, and A. I. Dyachenko, *JETP Lett.* **82**, 487 (2005).
- [17] V. E. Zakharov, A. O. Korotkevich, A. Pushkarev, and D. Resio, *Phys. Rev. Lett.* **99**, 164501 (2007).
- [18] A. O. Korotkevich, A. Pushkarev, D. Resio, and V. E. Zakharov, *Eur. J. Mech. B* **27**, 361 (2008).
- [19] S. Y. Annenkov and V. I. Shrira, *Phys. Rev. Lett.* **96**, 204501 (2006).
- [20] A. O. Korotkevich, *Phys. Rev. Lett.* **101**, 074504 (2008).
- [21] S. Nazarenko and S. Lukaschuk, *Annu. Rev. Condens. Matter Phys.* **7**, 61 (2016).
- [22] L. Deike, C. Laroche, and E. Falcon, *Europhys. Lett.* **96**, 34004 (2011).
- [23] E. Falcon and N. Mordant, *Annu. Rev. Fluid Mech.* **54**, 1 (2022).
- [24] E. Falcon, G. Michel, G. Prabhudesai, A. Cazaubiel, M. Berhanu, N. Mordant, S. Aumaître, and F. Bonnefoy, *Phys. Rev. Lett.* **125**, 134501 (2020).
- [25] A. O. Korotkevich, *Math. Comput. Simul.* **82**, 1228 (2012).
- [26] E. A. Kartashova, *Physica (Amsterdam)* **54D**, 125 (1991).
- [27] E. Kartashova, *Europhys. Lett.* **97**, 30004 (2012).
- [28] A. I. Dyachenko, A. O. Korotkevich, and V. E. Zakharov, *JETP Lett.* **77**, 477 (2003).
- [29] S. V. Nazarenko, *J. Stat. Mech.* (2006) L02002.
- [30] A. O. Korotkevich, A. I. Dyachenko, and V. E. Zakharov, *Physica (Amsterdam)* **321-322D**, 51 (2016).
- [31] Z. Zhang and Y. Pan, *Phys. Rev. E* **106**, 044213 (2022).
- [32] S. Y. Annenkov and V. I. Shrira, *J. Fluid Mech.* **561**, 181 (2006).
- [33] A. O. Korotkevich, *JETP Lett.* **97**, 126 (2013).
- [34] T. Y. Sheffield and B. Rumpf, *Phys. Rev. E* **95**, 062225 (2017).

- [35] V. E. Zakharov, *J. Appl. Mech. Tech. Phys.* **9**, 190 (1968).
- [36] See Supplemental Material at <http://link.aps.org/supplemental/10.1103/PhysRevLett.130.264002> for a complete derivation of weakly nonlinear dynamical Hamiltonian equations for surface gravity waves over 3D ideal incompressible fluid; detailed information about the dependence of the constant in front of the proposed spectrum on the forcing amplitude; description of the final  $\eta$ - and  $\psi$ -surfaces files for all of the simulation runs.
- [37] V. E. Zakharov, On the theory of surface waves, Ph.D. thesis, Budker Institute for Nuclear Physics, Novosibirsk, USSR, 1967.
- [38] F. Dias, A. I. Dyachenko, and V. E. Zakharov, *Phys. Lett. A* **372**, 1297 (2008).
- [39] M. Frigo and S. G. Johnson, *Proc. IEEE* **93**, 216 (2005).
- [40] Otherwise the level of pumping and fluxes would strongly depend on the level of dissipation. Importance of such a mechanism was demonstrated in Refs. [17,18].
- [41] V. E. Zakharov, A. O. Korotkevich, and A. O. Prokofiev, *AIP Proc.* **CP1168** **2**, 1229 (2009).
- [42] A. O. Korotkevich, A. O. Prokofiev, and V. E. Zakharov, *JETP Lett.* **109**, 309 (2019).
- [43] If we would have a large enough dynamical range for development of a direct cascade, according to Ref. [20], it would result in different slopes for the direct cascade spectrum.
- [44] GNU Octave, Scientific Programming Language, <https://octave.org/> (1988–2022).
- [45] GNU Project, <http://gnu.org> (1984–2022).
- [46] Gnuplot, command-driven interactive function plotting program, <http://gnuplot.info> (1986–2022).
- [47] What are standard errors in Gnuplot fit function, [http://gnuplot.info/docs\\_5.5/loc7129.html](http://gnuplot.info/docs_5.5/loc7129.html) (1986–2022).
- [48] This is the harmonic closest to the region influenced by pumping which is present in all datasets for least square fits in Table I.
- [49] One of the factors which might be important is deviation of the dispersion relation from the linear theory in the presence of the condensate (according to Eq. (3), the slope of the inverse cascade spectrum directly depends on the power of dispersion relation  $\delta$ ). It was show in Ref. [33] that in the presence of condensate rotation of phase of harmonics in the inverse cascade region cannot be described with a reasonable accuracy only by linear dispersion relation for gravity waves. One can try to take into account the interaction with condensate, e.g., using Bogolyubov transformation like in the case of dilute Bose gas (see sections about degenerated almost ideal Bose gas in Refs. [50] or [51]).
- [50] I. E. D. Aleksey, A. Abrikosov, and Lev P. Gorkov, *Methods of Quantum Field Theory in Statistical Physics* (Fizmatgiz, Moscow, 1962).
- [51] E. M. Lifshitz and L. P. Pitaevskii, *Statistical Physics: Course of Theoretical Physics—Vol. 9* (Elsevier, New York, 1978).
- [52] Documentation for Gnuplot `fit` function recommends considering standard errors just as an estimation, as many assumptions were used which cannot be justified in our case.
- [53] Y. Zhu, B. Semisalov, G. Krstulovic, and S. Nazarenko, *Phys. Rev. E* **106**, 014205 (2022).
- [54] J. W. Banks, T. Buckmaster, A. O. Korotkevich, G. Kovačič, and J. Shatah, *Phys. Rev. Lett.* **129**, 034101 (2022).
- [55] P. Denissenko, S. Lukaschuk, and S. V. Nazarenko, *Phys. Rev. Lett.* **99**, 014501 (2007).
- [56] S. Lukaschuk, S. Nazarenko, S. McLelland, and P. Denissenko, *Phys. Rev. Lett.* **103**, 044501 (2009).
- [57] A. Griffin, G. Krstulovic, V. S. L'vov, and S. Nazarenko, *Phys. Rev. Lett.* **128**, 224501 (2022).
- [58] G. Falkovich, *Phys. Fluids* **6**, 1411 (1994).
- [59] M. Chertkov, C. Connaughton, I. V. Kolokolov, and V. V. Lebedev, *Phys. Rev. Lett.* **99**, 084501 (2007).
- [60] H. Xia, M. Shats, and G. Falkovich, *Phys. Fluids* **21**, 125101 (2009).
- [61] A. O. Korotkevich, S. V. Nazarenko, Y. Pan, and J. Shatah, [arXiv:2305.01930](https://arxiv.org/abs/2305.01930).
- [62] A. Pushkarev, D. Resio, and V. E. Zakharov, *Physica (Amsterdam)* **184D**, 29 (2003).